

# Electronic structure of the diatomic VO anion: A combined photoelectron-imaging spectroscopic and theoretical investigation

Shi-Bo Cheng,<sup>1,2,\*</sup> Christopher L. Harmon,<sup>2</sup> Huan Yang,<sup>3</sup> and A. W. Castleman, Jr.<sup>2,4,†</sup>

<sup>1</sup>*School of Chemistry and Chemical Engineering, Shandong University, Jinan 250100, People's Republic of China*

<sup>2</sup>*Department of Chemistry, The Pennsylvania State University, University Park, Pennsylvania 16802, USA*

<sup>3</sup>*School of Physics, Shandong University, Jinan 250100, People's Republic of China*

<sup>4</sup>*Department of Physics, The Pennsylvania State University, University Park, Pennsylvania 16802, USA*

(Received 27 September 2016; published 15 December 2016)

The electronic structure of the diatomic VO anion was explored by combining the photoelectron-imaging spectroscopy and high-level theoretical calculations. The electron affinity (EA) of VO is determined to be  $1.244 \pm 0.025$  eV from the vibrationally resolved photoelectron spectrum acquired at 532 nm. The anisotropy parameter ( $\beta$ ) for the EA defined peak is measured to be  $1.59 \pm 0.02$ , indicating that it is the  $9\sigma$  electron attachment leading to the formation of the ground state of  $\text{VO}^-$ . The present imaging experiment provides direct evidence that the ground state of  $\text{VO}^-$  is  $X^3\Sigma^-$  with a  $(3\pi)^4(8\sigma)^2(9\sigma)^2(1\delta)^2$  electron configuration, which resolves the significant discrepancy in previous experiment and theory. In addition, the molecular orbitals and bonding involved in the anionic VO cluster are also examined based on the present high-level theoretical calculations.

DOI: [10.1103/PhysRevA.94.062506](https://doi.org/10.1103/PhysRevA.94.062506)

## I. INTRODUCTION

Due to their significant roles in catalysis, surface chemistry, and magnetic materials, transition metal (TM) oxides have been subject to numerous recent experimental and theoretical investigations [1–16]. Vanadium oxides, in particular, are the most versatile metal oxide catalysts predominantly used in industrial catalytic processes [17,18], making the understanding of the nature of vanadium-oxygen bonds highly valuable. Experiments on metal oxides in the gas phase can provide valuable molecular models with which to explore the fundamental bonding mechanism and their dependence on electronic structure without the interference from solvation and other environmental factors [3,19–22].

As the simplest vanadium oxide cluster, diatomic VO is one of the most systematically investigated molecules among the TM oxide clusters due to their significance in astrophysics [23,24]. The electronic structure of VO has been extensively explored by both experimental and theoretical methods [23–33]. The ground state of the VO cluster has been unambiguously determined to be of  $^4\Sigma$  symmetry with a  $(3\pi)^4(8\sigma)^2(9\sigma)^1(1\delta)^2$  electron configuration [26]. Moreover, the spectroscopic constants and term energies of a number of excited states of VO, which are  $A'^4\Phi$ ,  $1^2\Delta$ ,  $A^4\Pi$ ,  $\alpha^2\Sigma^+$ ,  $B^4\Pi$ , etc., have also been located by employing high-resolution Fourier transform spectroscopy [23,25].

Compared with the extensive investigations on VO, knowledge about the electronic structure of the  $\text{VO}^-$  ion is lacking or even controversial [28,34–37]. Experimentally, Wu and Wang reported the photoelectron spectroscopic study of  $\text{VO}^-$  by using the magnetic-bottle time-of-flight (MTOF) spectrometer [28]. They proposed that the ground state of  $\text{VO}^-$  should be  $X^5\Pi$  with an electron configuration of  $(3\pi)^4(8\sigma)^2(9\sigma)^1(1\delta)^2(4\pi)^1$ . Subsequent theoretical cal-

culations, however, questioned that assignment, where all theoretical results, independent of the theoretical methods and basis sets used, support that the  $X^3\Sigma^-$  state with a  $(3\pi)^4(8\sigma)^2(9\sigma)^2(1\delta)^2$  electron configuration should be the ground state of  $\text{VO}^-$  rather than the  $X^5\Pi$  state [34–37]. Therefore, significant discrepancy exists in previous experiment and theory regarding what type of electron ( $4\pi$  or  $9\sigma$ ) is attached to the neutral VO giving rise to  $\text{VO}^-$ . To eliminate this contradiction, advanced photoelectron-imaging spectroscopy is considered as the most appropriate and straightforward approach, which can reveal the information of the atomic orbital from which the photodetachment takes place by detecting the angular distributions of the detached electrons [38–42]. Additionally, many theoretical studies attempted to reproduce the experimental EA of VO. All previous theoretical calculations, however, substantially underestimate it by about 0.54–0.14 eV depending on the levels of theory and basis sets used [30,34–36], demonstrating that it is indeed a challenge to precisely describe the electronic properties of the vanadium oxide clusters, even for the simplest diatomic VO [36].

In the present experiment, the photoelectron-imaging spectroscopy of the  $\text{VO}^-$  cluster was performed to detect the orbital symmetry of the detached electron. The present experimental results provide direct evidence that the extra electron occupies the  $9\sigma$  molecular orbital of the neutral VO forming the ground state of  $\text{VO}^-$ , which resolves the discrepancy in previous experiment and theory. The EA of VO was measured to be  $1.244 \pm 0.025$  eV according to the vibrationally resolved photoelectron spectrum (PES), which is consistent with the prior measurement [28]. Furthermore, high-level theoretical calculations were accomplished to optimize the lowest-energy geometries of the neutral and anionic VO clusters, to estimate the EA of VO, and to examine the occupied molecular orbitals of the  $\text{VO}^-$  cluster.

## II. EXPERIMENTAL SECTION

The experimental setup conducted in the present study has been described in detail previously [43,44], and only a brief

\*shibocheng@sdu.edu.cn

†awc@psu.edu

overview is presented herein. The diatomic  $\text{VO}^-$  cluster was generated in a laser vaporization (LaVa) cluster source, where the second-harmonic output of a Nd:YAG laser (532 nm) was used to ablate a  $\frac{1}{4}$ -in. pure vanadium rod. To obtain smaller oxide clusters, a high-purity helium gas (typically 50 psi) seeded with 5%  $\text{N}_2\text{O}$  was used as a carrier gas to react with laser-ablated V atoms [19]. The formed neutral and charged clusters were expanded through a conical nozzle, and then collimated by a skimmer. Subsequently, the anionic clusters were exacted and mass analyzed using a Wiley-McLaren time-of-flight (TOF) mass spectrometer [45], which is oriented perpendicular to the cluster beam. The anion detector (Burle Electro-Optics bipolar detector), which contains microchannel plates, a scintillator, and a photomultiplier tube, is assembled at the end of the TOF mass spectrometer. Thus, an anion mass spectrum can be recorded by measuring the time at which the anions reach and strike the detector. The velocity map imaging (VMI) system is located before the anion detector, which is perpendicular to the TOF mass spectrometer. The mass selection in the present experiments is achieved by determining the arrival time of the anion of interest at the photodetachment region, which is at the center of the first two electrodes of the three-electrode design of Eppink and Parker [39]. The first electrode, known as the repeller, is time delayed and pulsed in order to ensure that only electrons detached from the mass-selected anion are being sampled. The pulse is on the order of a few microseconds before and after the photodetachment laser arrival, ensuring a uniform field is present. The voltage is pulsed from ground to approximately -180 V, and is supplied using a fast switch (Directed Energy PVM-4210) with a 25-ns rise time. In the photodetachment experiments, mass-selected  $\text{VO}^-$  clusters were photodetached by the second-harmonic (532 nm) output of another Nd:YAG laser, and the produced electrons were accelerated toward a position-sensitive detector consisting of a microchannel plate (MCP) and a phosphor screen. After flying through a field-free region, which is shielded against stray magnetic fields by a  $\mu$ -metal tube, the photoelectrons are mapped onto the position-sensitive detector. The 2D (two-dimensional) images generated on the phosphor screen were recorded with a charge-coupled device (CCD) camera. Finally, the BASEX and PBASEX programs were used to reconstruct all the photoelectron images [46,47], which yielded similar results. Subsequently, the obtained pixel and energy distribution were calibrated using the known binding energies of  $\text{Bi}^-$  to get the PES of  $\text{VO}^-$  [48]. For the PES of  $\text{VO}^-$ , three repeated measurements were recorded to ensure the true signals.

### III. COMPUTATIONAL METHOD

Calculations of the optimized geometries and electronic structures of the anionic and neutral VO clusters were accomplished using the GAUSSIAN 09 program [49]. Different spin multiplicity states of the clusters were attempted to determine the ground-state geometries. The structures were fully optimized without symmetry constraints. In this study, the coupled cluster singles and doubles with perturbative contributions of connected triplets, CCSD(T) level of theory [50,51] was employed to optimize the lowest-energy geometries and estimate the adiabatic detachment energy (ADE) and vertical

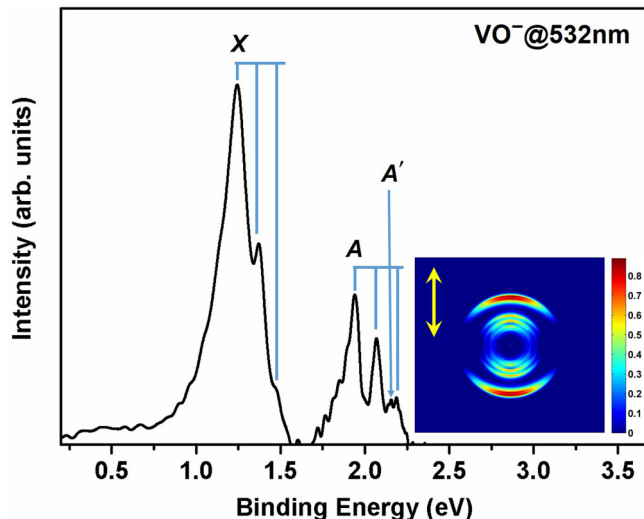


FIG. 1. Photoelectron image and the corresponding electron binding energy (BE) spectrum of the negatively charged VO cluster collected at 532 nm.

detachment energy (VDE) of the anionic VO cluster. This method has been proven to be an accurate theoretical approach to predict the geometrical and electronic properties of the TM doped clusters [52,53]. Throughout the calculations, the augmented correlation consistent triple-zeta (aug-cc-PVTZ) basis set was adopted for the oxygen atom [54,55], while the vanadium atomic orbital was described by the SDD (Stuttgart-Dresden effective core potential) with the Stuttgart-type small core (ten core electrons) and relativistic effective core potential (ECP) [56]. Moreover, vibration analyses were performed at the same level of theory to make sure that the optimized geometries are real minimum points and to take into account the zero-point energy correction. The theoretical ADE was defined as the energy difference between the optimized anionic and neutral structures, and the VDE was calculated by considering the energy difference between the ground state of the anion and the neutral cluster with the equilibrium geometry of the anion.

### IV. RESULTS AND DISCUSSION

Figure 1 depicts the photoelectron image and the corresponding PES of the  $\text{VO}^-$  cluster obtained at a photon energy of 2.33 eV (532 nm). In the present experiment, the laser polarization, which is represented by a double yellow arrow, is vertical in the image plane. The collected PES of  $\text{VO}^-$  reveals three major transition bands, which are labeled as X, A, and A'. The band X represents the EA defined transition, arising from the electronic transition between the ground state of  $\text{VO}^-$  and its corresponding neutral electronic ground state. A VDE of  $1.244 \pm 0.025$  eV is determined from the band maximum. In addition, obvious vibrational structure can be observed for the band X, which yields a vibrational frequency of  $964 \pm 60$   $\text{cm}^{-1}$  for the neutral VO cluster. Thus, in view of the vibrationally resolved PES, the ADE of the  $\text{VO}^-$  cluster is measured to be  $1.244 \pm 0.025$  eV, which is also the EA of VO. Another band (A) appears in the higher binding energy region with respect to

the transition  $X$ , and the VDE for this transition is measured to be  $1.939 \pm 0.025$  eV, which is consistent with the previously reported value  $1.927$  eV [28]. This band comes from the transition between the ground state of the anion and the doublet excited state ( $a^2\Sigma^-$ ) of the neutral [28]. Similarly, there also exists discernible vibrational structure in this band, yielding a vibrational frequency of  $1000 \pm 40$   $\text{cm}^{-1}$  for the  $a^2\Sigma^-$  excited state of VO. The energy spacing between the peaks  $X$  and  $A$ , which represents the splitting between the ground state ( $X^4\Sigma^-$ ) and the doublet excited state ( $a^2\Sigma^-$ ) of the neutral VO, is  $0.695$  eV. Besides these two bands ( $X$  and  $A$ ), the PES also discloses another peak ( $A'$ ) located at around  $2.156$  eV. This peak most likely comes from the transition between the ground state of the anion and the lowest quartet excited state ( $A'^4\Phi_{3/2}$ ) of the neutral VO cluster since the energy difference between the peaks  $X$  and  $A'$  ( $0.912$  eV) agrees with the term value of the  $A'^4\Phi_{3/2}$  state of VO ( $0.868$  eV) [24].

As mentioned above, significant discrepancy exists in previous experiment and theory regarding the electron configuration of the ground state of the anionic VO cluster [28,34–37]. Wu *et al.* assigned the  $X^5\Pi$  state as the ground state of  $\text{VO}^-$  [28], while the theoretical studies argued that the ground state should be the  $X^3\Sigma^-$  state [34–37]. One of the main motivations of the present study is to resolve such contradiction by employing photoelectron-imaging spectroscopy. As shown in Fig. 1, our photoelectron-imaging experiment defines the electronic transition from the anionic ground state to the ground state of VO (peak  $X$ ). Analysis of the anisotropy parameter ( $\beta$ ) of this peak provides valuable information as to the nature of the photodetached electron. It is well known that the Cooper-Zare formula [57] provides a quantitative description of the  $\beta$  parameter for partial wave emission from bound electronic states of definite orbital angular momentum as

$$\beta = \left[ l(l-1)\sigma_{l-1}^2 + (l+1)(l+2)\sigma_{l+1}^2 - 6l(l+1)\sigma_{l+1}\sigma_{l-1}\cos(\delta_{l+1} - \delta_{l-1}) \right] / 3(2l+1) \times \left[ l\sigma_{l-1}^2 + (l+1)\sigma_{l+1}^2 \right], \quad (1)$$

where  $l$  is the orbital angular momentum quantum number,  $\sigma_{l\pm 1}$  are the relative cross sections of the partial waves, and  $(\delta_{l+1} - \delta_{l-1})$  is the phase shift between these waves. Based on Eq. (1), detachment of an  $s$  electron leads to an outgoing  $p$  wave ( $l=1$ ) with maximum intensity parallel to the laser polarization and  $\beta = +2$ . In molecular systems, it is well accepted that detachment from the  $\sigma$  molecular orbital composed predominantly of atomic  $s$ -type character will produce an anisotropy parameter of  $\beta \sim 1.5$ – $2$  [58,59]. Thus, one could expect to obtain a  $\beta$  value close to  $2$  for the peak  $X$  (Fig. 1) if it is indeed the case that the extra electron enters into the  $9\sigma$  molecular orbital of VO to form the ground state ( $X^3\Sigma^-$ ) of  $\text{VO}^-$ . The experimentally measured  $\beta$  value associated with the  $X$  peak is  $1.59 \pm 0.02$ , demonstrating that the detachment process should occur from the  $9\sigma$  molecular orbital and the ground state of  $\text{VO}^-$  is the  $X^3\Sigma^-$  state. Moreover, as shown in Fig. 1, the photoelectron angular distribution (PAD) of the peak  $X$  is preferably oriented parallel to the laser polarization, which is also consistent with the character of the  $\sigma$  orbital detachment process. All these experimental findings, therefore, provide direct evidence that the ground state of  $\text{VO}^-$  is  $X^3\Sigma^-$  with

TABLE I. Theoretical equilibrium bond lengths  $r_e$ , vibrational frequencies  $\omega$ , and relative energies  $\Delta E$  for different spin multiplicities of the neutral and anionic VO clusters calculated at the CCSD(T) level of theory.

Species	Spin multiplicity	$r_e$ (Å)	$\omega$ ( $\text{cm}^{-1}$ )	$\Delta E$ (eV)
VO	2	1.560	1278.6	0.89
	4	1.583	947.9	0.00
	6	1.850	627.2	3.43
	8	2.638	115.7	6.44
$\text{VO}^-$	1	1.617	1003.4	1.04
	3	1.615	1046.4	0.00
	5	1.630	780.2	0.85
	7	1.985	471.2	3.75

a  $(3\pi)^4(8\sigma)^2(9\sigma)^2(1\delta)^2$  electron configuration, resolving the previous significant discrepancy.

To better understand the electronic structure and bonding of the anionic VO cluster, we performed high-level theoretical calculations to obtain the lowest-energy geometries of the studied clusters. Different spin states of the clusters were calculated, and the theoretical results are listed in Table I. As shown in Table I, the present calculations predict a quartet state as the global minimum of VO, while that of  $\text{VO}^-$  has a triplet spin multiplicity, which also supports the experimentally assigned ground-state electronic configuration of  $\text{VO}^-$  discussed above. It is necessary to note that the equilibrium bond length of  $^4\text{VO}$  is calculated to be about  $1.583$  Å, which is in excellent agreement with the experimental value of  $1.589$  Å [60], indicating that the theoretical method used here can provide accurate information about the properties of the vanadium oxide clusters. Additionally, the calculated vibrational frequency of  $^4\text{VO}$  is  $947.9$   $\text{cm}^{-1}$  (Table I), which agrees well with the measured value ( $964 \pm 60$   $\text{cm}^{-1}$ ) obtained in the present experiment. As for the ground state of  $\text{VO}^-$ , its bond length is calculated to be  $1.615$  Å. In addition, as shown in Table I, the low-lying quintet and singlet states of  $\text{VO}^-$  are less stable than the triplet state by  $0.85$  and  $1.04$  eV, respectively.

With the aid of optimized ground-state geometries of the neutral and anionic VO clusters, we can theoretically predict the ADE and VDE values of the  $\text{VO}^-$  cluster, which can be used to compare with the experimentally determined data. Such a comparison is of great value to test the accuracy of the chosen theoretical method and the optimized geometries. Additionally, as mentioned earlier, it is a challenge to precisely predict the EA of VO since there are relatively large differences between previous experiment and theory [34–36]. It has been demonstrated and emphasized that the energy levels of TM doped clusters are very sensitive to the choice of the level of theory and basis set [61]. Therefore, apart from determining the ground state of  $\text{VO}^-$ , another motivation of the present study is to explore an accurate theoretical method and level that can better describe the electronic properties of vanadium oxide clusters. According to the present calculations, the theoretical ADE and VDE of the  $\text{VO}^-$  cluster are  $1.215$  and  $1.230$  eV, respectively, which are summarized in Table II. It is worth noting that the calculated ADE and VDE values are in good agreement with the experimentally measured data deviating

TABLE II. Experimental and theoretical ADE and VDE of the  ${}^3\text{VO}^-$  cluster. Previous theoretical results are also included for comparison.

Species	ADE (eV)			VDE (eV)		
	Expt.	Theor.		Expt.	Theor.	
		This work <sup>a</sup>	Previous <sup>b</sup>		This work <sup>a</sup>	Previous <sup>b</sup>
${}^3\text{VO}^-$	1.244(25) <sup>c</sup>	1.215	1.031/1.091 <sup>d</sup> 0.81/0.98/1.09 <sup>e</sup> 0.85/0.83 <sup>f</sup> 1.05/1.09/1.03/0.72/0.69 <sup>g</sup>	1.244(25) <sup>c</sup>	1.230	1.039/1.100 <sup>e</sup> 0.86/0.83 <sup>f</sup>

<sup>a</sup>Current theoretical ADE and VDE values of the  $\text{VO}^-$  cluster calculated at the CCSD(T) level of theory.

<sup>b</sup>Previous theoretical results for the ADE and VDE of  $\text{VO}^-$ . The values divided by slash represent the results calculated at different levels of theory and basis sets.

<sup>c</sup>Numbers in the parentheses represent experimental uncertainties in the last two digits, which are obtained by calculating the standard deviation of multiple measurements.

<sup>d</sup>Reference [30].

<sup>e</sup>Reference [34].

<sup>f</sup>Reference [35].

<sup>g</sup>Reference [36].

by just 2% and 1% from those of  $\text{VO}^-$ , respectively. The theoretical results from previous studies are also included in Table II for comparison [30,34–37]. As evidenced in Table II, the present theoretical results are much closer to the experimental data than previous ones. This demonstrates that the level of theory and basis set used here is more appropriate to predict the electronic properties of  $\text{VO}^-$  than prior ones. We recommend that the theoretical level used here may also be an accurate method to predict the physicochemical properties of other TM doped clusters.

To get more insights in the molecular orbitals (MOs) and bonding of the anionic VO cluster, we have calculated the occupied valence Kohn-Sham MOs of the  $\text{VO}^{0/-1}$  clusters, which are displayed in Fig. 2. As shown in Fig. 2, the extra electron occupies the highest occupied molecular orbital (HOMO) ( $9\sigma$ ) of the neutral VO to form the anion, supporting the experimentally observed  $\beta$  value ( $1.59 \pm 0.02$ ) and the triplet character of the ground state of  $\text{VO}^-$ . Based on the present calculations (Fig. 2), HOMO-1 and HOMO-2 of  $\text{VO}^-$  are occupied  $3\pi$  MOs with the electron clouds mainly located on the  $2p_y$  and  $2p_x$  atomic orbitals (AOs) of the oxygen atom, respectively. Another two MOs in  $\text{VO}^-$ , which are HOMO-3 and HOMO-4, are singly occupied, the origins giving rise to the magnetic characteristics of the  $\text{VO}^-$  cluster. These two  $\delta$ -type MOs are predominantly composed of the  $3d_{xy}$  and  $3d_{x^2-y^2}$

AOs of V, respectively. Additionally, HOMO-5 of  $\text{VO}^-$  has  $8\sigma$  orbital symmetry resulting from the overlap between the  $3d_{z^2}$  AO on V and the  $2p_z$  AO on O. As for the  $9\sigma$  orbital in  $\text{VO}^-$ , it mainly comprises the  $4s$  AO of V and the  $2s$  AO of O. As can be seen from Fig. 2, this  $\sigma$  MO features antibonding character, which is similar to valence  $\sigma$  orbitals in ZrSi ( $2\sigma$  orbital of the  ${}^2\Sigma^+$  state) and TiSi ( $11\sigma$  orbital of the  ${}^5\Delta$  ground state) [62,63]. The attachment of the extra electron in this  $\sigma$  orbital leading to the formation of the ground state of  $\text{VO}^-$  may explain the elongation of the V-O bond length in  $\text{VO}^-$ .

## V. CONCLUSIONS

In conclusion, we reported a photoelectron-imaging spectrum of the anionic VO cluster at a photon energy of 2.33 eV (532 nm). The observed PES possesses obvious vibrational structures, from which the EA of VO was measured to be  $1.244 \pm 0.025$  eV. The PAD for the EA defined peak and high-level theoretical calculations were employed to determine the ground state of the VO anion. The present experimental and theoretical findings provide direct evidence that the ground state of  $\text{VO}^-$  is  $X^3\Sigma^-$  with a  $(3\pi)^4(8\sigma)^2(9\sigma)^2(1\delta)^2$  electron configuration rather than the  $X^5\Pi$  state, resolving the significant contradiction in previous experiment and theory. Additionally, the theoretical ADE and VDE values of  $\text{VO}^-$  were calculated at the CCSD(T) level of theory, yielding highly accurate results. This implies that the level of theory and basis set used here can better describe the electronic properties of vanadium oxide clusters, which may be also suitable for predicting accurate properties of other TM oxide clusters.

## ACKNOWLEDGMENTS

This material is based upon work supported by the Air Force Office of Science Research under AFOSR Award No. FA9550-10-1-0071, the National Natural Science Foundation of China (NSFC) (Grant No. 21603119), and the Natural Science Foundation of Shandong Province (Grant No. ZR2016BQ09).

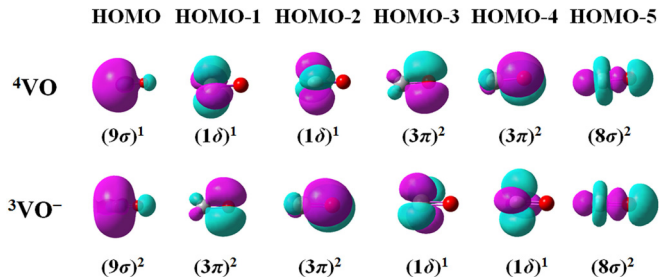


FIG. 2. 3D plots of select occupied valence Kohn-Sham molecular orbitals (MOs) describing the bonding in the neutral and anionic VO species. The MOs' isosurface value is 0.03 au.

- [1] V. E. Henrich and P. A. Cox, *The Surface Science of Metal Oxides* (Cambridge University Press, Cambridge, UK, 1994).
- [2] C. N. R. Rao, *Annu. Rev. Phys. Chem.* **40**, 291 (1989).
- [3] P. Ferstl, L. Hammer, C. Sobel, M. Gubo, K. Heinz, M. A. Schneider, F. Mittendorfer, and J. Redinger, *Phys. Rev. Lett.* **117**, 046101 (2016).
- [4] K. S. Molek, C. Anfuso-Cleary, and M. A. Duncan, *J. Phys. Chem. A* **112**, 9238 (2008).
- [5] V. Bonačić-Koutecký, R. Mitrić, U. Werner, L. Wöste, and R. S. Berry, *Proc. Natl. Acad. Sci. USA* **103**, 10594 (2006).
- [6] R. S. Berry and B. M. Smirnov, *Phys. Rep.* **527**, 205 (2013).
- [7] Z. Zhong and P. Hansmann, *Phys. Rev. B* **93**, 235116 (2016).
- [8] H. J. Zhai, C. Bürgel, V. Bonačić-Koutecký, and L. S. Wang, *J. Am. Chem. Soc.* **130**, 9156 (2008).
- [9] P. Calaminici, A. M. Köster, and D. R. Salahub, *J. Chem. Phys.* **118**, 4913 (2003).
- [10] P. Calaminici, R. Flores-Moreno, and A. M. Köster, *J. Chem. Phys.* **121**, 3558 (2004).
- [11] S. G. Ard, J. J. Melko, O. Martinez, Jr., V. G. Ushakov, A. Li, R. S. Johnson, N. S. Shuman, H. Guo, J. Troe, and A. A. Viggiano, *J. Phys. Chem. A* **118**, 6789 (2014).
- [12] D. Preziosi, M. Alexe, D. Hesse, and M. Salluzzo, *Phys. Rev. Lett.* **115**, 157401 (2015).
- [13] J. B. Kim, M. L. Weichman, and D. M. Neumark, *J. Chem. Theory Comput.* **10**, 5235 (2014).
- [14] J. B. Kim, M. L. Weichman, and D. M. Neumark, *J. Am. Chem. Soc.* **136**, 7159 (2014).
- [15] T. Ichino, A. J. Gianola, D. H. Andrews, and W. C. Lineberger, *J. Phys. Chem. A* **108**, 11307 (2004).
- [16] W. J. Zheng, K. H. Bowen, Jr., J. Li, I. Dabkowska, and M. Gutowski, *J. Phys. Chem. A* **109**, 11521 (2005).
- [17] B. M. Weckhuysen, and D. E. Keller, *Catal. Today* **78**, 25 (2003).
- [18] G. C. Bond and S. F. Tahir, *Appl. Catal.* **71**, 1 (1991).
- [19] S. Cheng, C. Berkdemir, J. J. Melko, and A. W. Castleman, Jr., *J. Phys. Chem. A* **117**, 11896 (2013).
- [20] J. E. Mann, S. E. Waller, and C. C. Jarrold, *J. Phys. Chem. A* **117**, 12116 (2013).
- [21] X. Yang, T. Waters, X. B. Wang, R. A. J. O'Hair, A. G. Wedd, J. Li, D. A. Dixon, and L. S. Wang, *J. Phys. Chem. A* **108**, 10089 (2004).
- [22] Z. L. Liu, H. Xie, Q. J. Li, Z. B. Qin, R. Cong, X. Wu, Z. C. Tang, and H. J. Fan, *J. Chem. Phys.* **140**, 034312 (2014).
- [23] A. J. Merer, *Annu. Rev. Phys. Chem.* **40**, 407 (1989).
- [24] A. J. Merer, G. Huang, A. S. C. Cheung, and A. W. Taylor, *J. Mol. Spectrosc.* **125**, 465 (1987), and references therein.
- [25] A. S. C. Cheung, P. G. Hajigeorgiou, G. Huang, S. Z. Huang, and A. J. Merer, *J. Mol. Spectrosc.* **163**, 443 (1994).
- [26] P. H. Kasai, *J. Chem. Phys.* **49**, 4979 (1968).
- [27] A. S. C. Cheung, A. W. Taylor, and A. J. Merer, *J. Mol. Spectrosc.* **92**, 391 (1982).
- [28] H. Wu and L. S. Wang, *J. Chem. Phys.* **108**, 5310 (1998).
- [29] J. C. Rienstra-Kiracofe, G. S. Tschumper, H. F. Schaefer III, S. Nandi, and G. B. Ellison, *Chem. Rev.* **102**, 231 (2002).
- [30] B. Dai, K. Deng, J. Yang, and Q. Zhu, *J. Chem. Phys.* **118**, 9608 (2003).
- [31] E. G. Bakalbassis, M-A. D. Stiakaki, A. C. Tshipis, and C. A. Tshipis, *Chem. Phys.* **205**, 389 (1996).
- [32] M. Dolg, U. Wedig, H. Stoll, and H. Preuss, *J. Chem. Phys.* **86**, 2123 (1987).
- [33] C. W. Bauschlicher, Jr. and S. R. Langhoff, *J. Chem. Phys.* **85**, 5936 (1986).
- [34] G. L. Gutsev, B. K. Rao, and P. Jena, *J. Phys. Chem. A* **104**, 5374 (2000).
- [35] S. F. Vyboishchikov and J. Sauer, *J. Phys. Chem. A* **104**, 10913 (2000).
- [36] M. Pykavy and C. van Wüllen, *J. Phys. Chem. A* **107**, 5566 (2003).
- [37] E. Miliordos and A. Mavridis, *J. Phys. Chem. A* **111**, 1953 (2007).
- [38] R. Mabbs, E. R. Grumbling, K. Pichugin, and A. Sanov, *Chem. Soc. Rev.* **38**, 2169 (2009).
- [39] A. T. J. B. Eppink and D. H. Parker, *Rev. Sci. Instrum.* **68**, 3477 (1997).
- [40] S. B. Cheng, C. Berkdemir, J. J. Melko, and A. W. Castleman, Jr., *J. Am. Chem. Soc.* **136**, 4821 (2014).
- [41] S. B. Cheng, C. Berkdemir, and A. W. Castleman, Jr., *Phys. Chem. Chem. Phys.* **16**, 533 (2014).
- [42] S. B. Cheng, C. Berkdemir, and A. W. Castleman, Jr., *Proc. Natl. Acad. Sci. USA* **112**, 4941 (2015).
- [43] K. L. Knappenberger, C. E. Jones, M. A. Sobhy, and A. W. Castleman, Jr., *Rev. Sci. Instrum.* **77**, 123901 (2006).
- [44] M. A. Sobhy, J. U. Reveles, U. Gupta, S. N. Khanna, and A. W. Castleman, Jr., *J. Chem. Phys.* **130**, 054304 (2009).
- [45] W. C. Wiley and I. H. McLaren, *Rev. Sci. Instrum.* **26**, 1150 (1955).
- [46] V. Dribinski, A. Ossadtchi, V. A. Mandelshtam, and H. Reisler, *Rev. Sci. Instrum.* **73**, 2634 (2002).
- [47] G. A. Garcia, L. Nahon, and I. Powis, *Rev. Sci. Instrum.* **75**, 4989 (2004).
- [48] T. Andersen, H. K. Haugen, and H. Hotop, *J. Phys. Chem. Ref. Data* **28**, 1511 (1999).
- [49] M. J. Frisch *et al.*, GAUSSIAN 09, revision B.01 (Gaussian Inc., Wallingford, CT, 2009).
- [50] G. D. Purvis III and R. J. Bartlett, *J. Chem. Phys.* **76**, 1910 (1982).
- [51] K. Raghavachari, G. W. Trucks, J. A. Pople, and M. Head-Gordon, *Chem. Phys. Lett.* **157**, 479 (1989).
- [52] S. B. Cheng and A. W. Castleman, Jr., *J. Phys. Chem. A* **118**, 6935 (2014).
- [53] Q. Y. Liu, L. Hu, Z. Y. Li, C. G. Ning, J. B. Ma, H. Chen, and S. G. He, *J. Chem. Phys.* **142**, 164301 (2015).
- [54] T. H. Dunning, Jr., *J. Chem. Phys.* **90**, 1007 (1989).
- [55] R. A. Kendall, T. H. Dunning, Jr., and R. J. Harrison, *J. Chem. Phys.* **96**, 6796 (1992).
- [56] M. Dolg, U. Wedig, H. Stoll, and H. Preuss, *J. Chem. Phys.* **86**, 866 (1987).
- [57] J. Cooper and R. N. Zare, *J. Chem. Phys.* **48**, 942 (1968).
- [58] P. G. Wenthold, R. F. Gunion, and W. C. Lineberger, *Chem. Phys. Lett.* **258**, 101 (1996).
- [59] S. J. Peppernick, K. D. D. Gunaratne, and A. W. Castleman, Jr., *Proc. Natl. Acad. Sci. USA* **107**, 975 (2010).
- [60] K. P. Huber and G. Herzberg, *Constants of Diatomic Molecules* (Van Nostrand-Reinhold, New York, 1979).
- [61] J. F. Harrison, *Chem. Rev.* **100**, 679 (2000).
- [62] K. D. D. Gunaratne, A. Hazra, and A. W. Castleman, Jr., *J. Chem. Phys.* **134**, 204303 (2011).
- [63] M. Tomonari and K. Tanaka, *Theor. Chem. Acc.* **106**, 188 (2001).